# Effect of side-chains on solution properties of *N*-(2-hydroxypropyl)methacrylamide copolymers in aqueous solvents

**Č. Koňák*, R. C. Rathi, P. Kopečková and J. Kopeček†**
*Department of Pharmaceutics and Pharmaceutical Chemistry/CCCD, and Department of Bioengineering, University of Utah, Salt Lake City, UT 84112, USA*
*(Received 7 May 1992; revised 23 February 1993)*

The solubility and association of water-soluble copolymers of *N*-(2-hydroxypropyl)methacrylamide (HPMA) containing both *p*-nitroaniline-terminated oligopeptide side-chains and *N*-2-hydroxyethylpiperazine-*N'*-ethanesulfonic acid (HEPES) side-chains in aqueous solvents were investigated using light scattering methods. The weight-average molar masses, second virial coefficients, diffusion coefficients and hydrodynamic sizes of the copolymer molecules and their aggregates were studied as a function of the copolymer concentration, temperature and solvent pH. The copolymers with a low content (<2 mol%) of hydrophobic side-chains terminated in *p*-nitroaniline were soluble molecularly in aqueous solutions. The water solubility was substantially enhanced by the presence of HEPES side-chains. The copolymers with a high content (~7 mol%) of *p*-nitroaniline-containing side-chains associated in water, generally forming two types of micelles of different sizes. Micelle formation depended on hydrophobic and amphiphilic side-chain content, polymer concentration, temperature and solvent pH. Thus, macromolecules containing a higher amount of *p*-nitroaniline and a small amount of HEPES side-chains tended to form small, compact micelles with the hydrophobic *p*-nitroaniline molecules oriented into the core, while macromolecules with a high content of HEPES side-chains tended to form large micelles. The formation of large micelles was strongly dependent on solvent pH, due to the electrolyte behaviour of the HEPES moieties. The solution properties of the copolymers generally reflected the competition between these two association processes.

**(Keywords: amphiphilic side-chains; copolymers; micelles)**

## INTRODUCTION

Water-soluble synthetic or natural polymers have been proposed as targetable carriers of biologically active compounds[1]. Attaching the biologically active compound (drug) to the polymer molecule changes the mechanism of interaction between the drug and the living organism on a cellular level[2]. For example, copolymers of *N*-(2-hydroxypropyl)methacrylamide (HPMA) containing oligopeptide side-chains terminated in anticancer drugs have been developed as targetable polymeric drug carriers[3]. Since most drugs are hydrophobic, upon binding to a hydrophilic polymer carrier the solubility behaviour of the polymer changes, e.g. the phase separation is shifted to lower temperature values. Since a conjugate of hydrophilic polymers with hydrophobic compounds possesses amphiphilic properties in aqueous solutions[4], association or aggregation phenomena have been observed[5–7]. In our earlier paper[5], the solution properties of water-soluble copolymers of HPMA containing oligopeptide side-chains terminated in *p*-nitroaniline (drug model) were studied using light scattering, g.p.c. and sedimentation methods. It was found that these copolymers associated in water forming micelles with the hydrophobic side-chains oriented into the core, while the hydrophilic polymer chains formed the shell of the spherical micelles. The association number and compactness of the micelles were dependent on the hydrophobic side-chain content, polymer concentration and temperature. Recently, association behaviour of this type was observed in aqueous solutions of poly(L-glutamic acid) with bound hydrophobic adriamycin[6].

The objective of this study was to increase the water solubility of HPMA copolymers containing hydrophobic side-chains through copolymerization with the acryloyl ester of *N*-2-hydroxyethylpiperazine-*N'*-2-ethanesulfonic acid (AHEPES). Copolymers of HPMA with different amounts of *N*-methacryloylglycylleucylphenylalanine *p*-nitroanilide (MA-Gly-Leu-Phe-NAp) and the acryloyl ester of *N*-2-hydroxyethylpiperazine-*N'*-2-ethanesulfonic acid sodium salt were synthesized (*Scheme 1*). The relations between the structure of the HPMA copolymers and their solubility and association in different buffers were investigated by light scattering methods. The weight-average molar masses, second virial coefficients, diffusion coefficients and hydrodynamic sizes of copolymer molecules and their aggregates were studied as a function of the copolymer concentration, temperature and solvent pH.

* Present address: Institute of Macromolecular Chemistry, Czech Academy of Sciences, Heyrovský Sq. 2, 16206 Prague 6, Czech Republic
† To whom correspondence should be addressed at the Department of Bioengineering, 2480 MEB, University of Utah, Salt Lake City, UT 84112, USA

0032-3861/93/224767-07

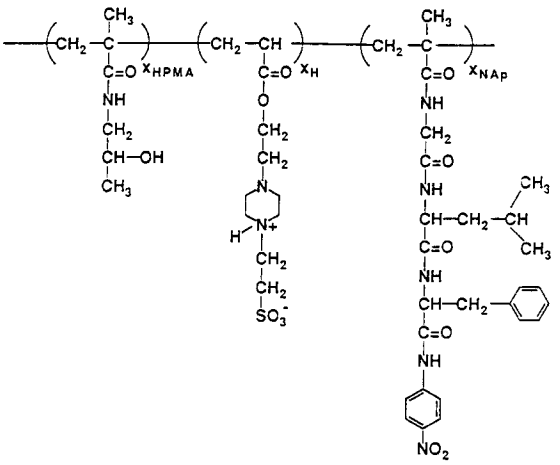

**Scheme 1** Chemical structure of HPMA copolymers; $x_H$, $x_{NAp}$ and $x_{HPMA}$ are the contents of AHEPES, MA-Gly-Leu-Phe-NAp and HPMA comonomers, respectively

## EXPERIMENTAL

### *Abbreviations*

AHEPES acryloyl ester of *N*-2-hydroxyethylpiperazine-*N'*-2-ethanesulfonic acid
AIBN 2,2'-azobisisobutyronitrile
DCC *N,N'*-dicyclohexylcarbodiimide
DMF dimethylformamide
DMSO dimethylsulfoxide
HEPES *N*-2-hydroxyethylpiperazine-*N'*-2-ethanesulfonic acid
HPMA *N*-(2-hydroxypropyl)methacrylamide
MA-Gly-Leu-Phe-NAp *N*-methacryloylglycylleucylphenylalanine *p*-nitroanilide
TRIS 2-amino-2-hydroxymethyl-1,3-propanediol
$x_H$, $x_{HPMA}$, $x_{NAp}$ molar fractions of AHEPES, HPMA and MA-Gly-Leu-Phe-NAp monomer units in the copolymers, respectively.

### *Materials*

HPMA was prepared according to previously described procedures[8]. AIBN was recrystallized from methanol. Solvents were freshly distilled. Sodium hydride was obtained from the Aldrich Chemical Co. (Milwaukee, WI, USA) as a 97% dispersion in oil. Glycylleucine, phenylalanine *p*-nitroanilide and HEPES sodium salt were from the Sigma Chemical Co. (St. Louis, MO, USA).

*Buffers.* Potassium hydrogen phthalate (0.05 M), pH 3.0 and 4.0; potassium dihydrogen phosphate (0.05 M), pH 6.0 and 8.0; sodium bicarbonate (0.025 M), pH 10; TRIS (0.05 M) + NaCl (0.5 M), pH 8.0.

### *Synthesis of monomers*

*AHEPES.* AHEPES was synthesized by a modification of the procedure of Mulvaney *et al.*[9]: m.p. 208°C (ref. 9, 200°C).

I.r. (KBr): 1725, 1625, 820 $cm^{-1}$.

$^1H$ n.m.r.: (200 MHz, $D_2O$); $\delta = 2.3$–$2.8$ (m, 12H); 3.0 (m, 2H); 4.2 (t, 2H); 5.85 (d, 1H); 6.1 (m, 1H); 6.3 (d, 1H).

Analysis: calculated for $C_{11}H_{19}N_2O_5NaS$: C, 42.03%; H, 6.05%; N, 8.91%; S, 10.19%. Found: C, 41.99%; H, 6.08%; N, 8.89%; S, 10.10%.

*MA-Gly-Leu-Phe-NAp.* (i) *N*-Methacryloylglycylleucine was synthesized as previously described[10].

(ii) MA-Gly-Leu-Phe-NAp: *N*-methacryloylglycylleucine (0.640 g, $2.50 \times 10^{-3}$ mol) and phenylalanine *p*-nitroanilide (0.783 g, $2.75 \times 10^{-3}$ mol) were dissolved in dry DMF (10 ml) and cooled to −10°C. A solution of DCC (0.566 g, $2.75 \times 10^{-3}$ mol) in dry DMF (5 ml) was added dropwise with vigorous stirring and cooling. The reaction mixture was stirred for 3 h at −10°C, 3 h at 0°C and then for 2 days at room temperature. A few drops of glacial acetic acid were added to destroy the excess of DCC, and the reaction mixture was stirred for an additional 1 h at room temperature. The dicyclohexyl urea that precipitated was filtered, and the DMF was evaporated under vacuum. The residue was dissolved in ethyl acetate, filtered, washed with saturated sodium bicarbonate and dried over $MgSO_4$. The solution was evaporated to dryness and recrystallized from ethyl acetate to give 0.64 g (48%) of MA-Gly-Leu-Phe-NAp: m.p. 184°C; ($\varepsilon_{330} = 1.4 \times 10^4$ in DMSO).

I.r. (KBr): 3270, 1650, 1620, 1550, 1530, 860 $cm^{-1}$.

$^1H$ n.m.r.: (200 MHz, $CDCl_3$ + DMSO-$d_6$); $\delta = 0.85$ (d, d, 6H); 1.4 (m, 2H); 1.8 (s, 3H); 3.2 (m, 2H); 3.6 (m, 2H); 4.1 (m, 1H); 4.8 (m, 1H); 5.2 (s, 1H); 5.7 (s, 1H); 7.3 (m, 5H); 8.1 (m, 4H); 8.7 (d, 1H); 9.3 (s, 1H).

Analysis: calculated for $C_{27}H_{33}N_5O_6$: C, 61.95%; H, 6.30%; N, 13.38%. Found: C, 61.83%; H, 6.38%, N, 13.31%.

### *Synthesis and characterization of HPMA copolymers*

Copolymers were prepared by free-radical precipitation copolymerization[10] of HPMA, AHEPES sodium salt and MA-Gly-Leu-Phe-NAp in acetone containing a small amount of DMSO (to dissolve the monomer mixture) at 50°C for 24 h using AIBN as the initiator. The ratio of monomers to initiator and solvent was 12.5:0.6:86.9 wt%. The stoichiometry of the monomers in the feed was manipulated to afford a variety of HPMA copolymers containing different amounts of HEPES and *p*-nitroaniline side-chains (*Scheme 1*). The copolymers were purified by dialysis against water for 2 days and lyophilized.

The amount of *p*-nitroaniline-terminated side-chains in the copolymers was determined with u.v. spectrophotometry ($\lambda_{max} = 330$ nm in DMSO). The AHEPES content of the copolymers was determined by sulfur analysis (*Table 1*).

### *Static light scattering*

Static light scattering (s.l.s.) measurements were performed with a Brookhaven goniometer equipped with

**Table 1** Molecular characteristics of HPMA copolymers

| Sample | $x_H$[a] (mol%) | $x_{NAp}$[b] (mol%) | $dn/dc$[c] (ml $g^{-1}$) | $M_w \times 10^{-4}$ (g $mol^{-1}$) |
|---|---|---|---|---|
| 1 | 0 | 0.0 | 0.135 | 11.4 |
| 1a | 0 | 1.1 | 0.135 | 3.2 |
| 1b | 0 | 2.7 | 0.135 | 2.9 |
| 1c | 0 | 5.6 | 0.135 | 2.8 |
| 1d | 0 | 7.0 | 0.135 | 2.8 |
| 2 | 9.2 | 0.0 | 0.133 | 1.5 |
| 2a | 9.6 | 1.1 | 0.133 | 1.3 |
| 2b | 9.4 | 3.0 | 0.133 | 1.3 |
| 2c | 9.4 | 5.9 | 0.133 | 1.4 |
| 2d | 8.9 | 6.5 | 0.133 | 1.4 |
| 3 | 18.2 | 7.4 | 0.130 | 1.3 |
| 4 | 35.9 | 6.8 | 0.127 | 1.4 |

[a] Amount of AHEPES in the copolymer
[b] Amount of MA-Gly-Leu-Phe-NAp in the copolymer
[c] Refractive index increment determined in 2-ethoxyethanol

**Table 2** Characteristics[a] of HPMA copolymers in TRIS buffer solutions

| Sample | $(dn/dc)_\mu$ (ml g$^{-1}$) | $M_w^l$ (g mol$^{-1}$) | $A_2 \times 10^5$ (ml g$^{-2}$ mol) | $R_{hs}$ (nm) | $R_{hl}$ (nm) | $A_l/A_s$ | $n$ | $T_c$ (°C) |
|---|---|---|---|---|---|---|---|---|
| 1 | 0.146 | 123000 | 26 | 9.5 | – | 0 | ~1 | – |
| 1a | 0.146 | 37000 | 18 | 5.0 | – | 0 | ~1 | – |
| 1b | 0.146 | 84000 | 4.5 | 6.3 | – | <0.05 | 2.9 | – |
| 1c | 0.146 | 147000 | −0.7 | 6.9 | – | <0.1 | 5.3 | – |
| 1d | 0.146 | 440000 | −0.4 | 7.9 | 43 | 0.71 | 16 | 33.5 |
| 2 | 0.144 | 39000 | 63 | 4.9 | – | 0 | 2.6 | – |
| 2a | 0.144 | 33000 | 32 | 5.2 | – | 0 | 2.9 | – |
| 2b | 0.144 | 64000 | 24 | 4.6 | – | 0 | 4.8 | – |
| 2c | 0.144 | 92000 | 9.5 | 4.7 | – | 0 | 6.6 | – |
| 2d | 0.144 | 110000 | 3.5 | 5.4 | – | <0.1 | 8.1 | 72.5 |
| 3 | 0.143 | 95000 | 2.3 | 5.1 | 35 | 0.12 | 7.3 | 79 |
| 4 | 0.139 | 53000 | 13 | 4.3 | 43 | 0.21 | 3.8 | 68 |

[a] $(dn/dc)_\mu$, effective value of the refractive index increment; $M_w^l$, weight-average molecular mass (micelles + unimers); $A_2$, second virial coefficient; $R_{hs}$, hydrodynamic radius of smaller aggregates; $R_{hl}$, hydrodynamic radius of larger aggregates; $A_l$, relative scattering amplitude of the slow diffusion process (for $c = 0.01$ g ml$^{-1}$); $A_s$, relative scattering amplitude of the fast diffusion process (for $c = 0.01$ g ml$^{-1}$); $n$, association number; $T_c$, temperature of macrophase separation

an argon laser (vertically polarized, $\lambda = 514.5$ nm) at 22°C. The data obtained on the copolymer solutions in the TRIS buffer were processed in the form of the equation:

$$Kc/\Delta R(0) = 1/M_w + 2A_2c$$

where $M_w$ is the weight-average molar mass, $K$ is the optical constant which includes the square of the refractive index increment, $A_2$ is the second virial coefficient, $c$ is concentration and $\Delta R(0)$ is the excess Rayleigh ratio, proportional to the intensity of light scattered from the copolymer solution, extrapolated to zero scattering angle. Refractive index increments of copolymer solutions were measured with a model RF-600 differential refractometer manufactured by C. N. Wood Mfg Co. (*Tables 1* and *2*). For the TRIS buffer solutions an effective value of the refractive index increment $(dn/dc)_\mu$ was determined after dialysis of copolymer solutions against the buffer, as described in ref. 11.

2-Ethoxyethanol, a good solvent for all copolymers, was employed for molecular characterization of the copolymers. The light scattering data were treated by the standard Zimm method.

*Dynamic light scattering*

Dynamic light scattering (d.l.s.) measurements were performed using a standard multiangle Brookhaven Instruments spectrometer with an argon ion laser and a 78 channel BI 2030 (Brookhaven Instruments), multibit, multitau autocorrelator operating with four simultaneous sampling times covering 4.5 decades in delay time. The samples were thermostatted in a refractive-index-matching liquid (toluene).

Two different methods were used to analyse the autocorrelation functions: (1) the method of cumulants using both the measured and floating baseline options and assuming homodyne detection; and (2) the multisampling time autocorrelation functions were analysed by inverse Laplace transform using the CONTIN[12] method of constrained regularization to obtain a distribution $A(\tau)$ of decay times. This method uses an equidistant logarithmic grid with fixed components (here a grid of 10 components per decade) and determines their amplitudes.

## RESULTS AND DISCUSSION

Multisampling time autocorrelation functions were measured for a series of HPMA copolymer samples with $x_H = 0$–100 mol% and $x_{NAp} = 0$–7.4 mol% at different concentrations. Since the autocorrelation functions of samples with $x_{NAp} \approx 7$ mol% (copolymers 1d, 2d, 3, 4) were not single-exponential (the quality of single-exponential fits was very low), they were analysed employing the CONTIN program. The corresponding distribution functions of decay times, $A(\tau)$, (the scattering angle $\theta = 90°$, $c = 0.01$ g ml$^{-1}$) are shown in *Figure 1* for three of the copolymers with fixed content of *p*-nitroaniline ($x_{NAp} \approx 7$ mol%), and different contents of HEPES side-chains. In all cases, the decay time distribution functions consisted of two well-separated bands with peaks at short and long decay times, $\tau_s$ and $\tau_l$, respectively. Thus, the contributing dynamic processes could be adequately reduced to two main components only. The long decay time peak was very weak in the case of copolymer 2d ($x_H = 8.9$ mol%). Both of these dynamic processes have diffusion character because both $\tau_s^{-1}$ and $\tau_l^{-1}$ were linearly dependent on $K^2$ ($K$ is the length of the scattering vector). Hence, it was possible to introduce and calculate two corresponding diffusion coefficients, $D_s$ $(= 1/2K^2\tau_s)$ and $D_l$ $(= 1/2K^2\tau_l)$. The existence of two diffusion coefficients in dilute solution generally pointed to the existence of at least two types of well-defined aggregates with different hydrodynamic diameters. The dynamic process corresponding to the fast coefficient ($D_s$) could only be found in copolymer solutions with $x_{NAp} < 6$ mol% (*Table 2*).

The concentration dependences of $D_s$ for copolymers 1d, 2d, 3, 4 with $x_{NAp} \approx 7$ mol% are plotted in *Figure 2*. The data show that $D_s$ was strongly dependent on $x_H$: $D_s$ decreased with increasing $x_H$. As for concentration dependence, $D_s$ was a linear function of concentration at higher concentrations and increased with decreasing concentration at low concentrations. The slope of the concentration dependence of $D_s$ for $c \geq 5 \times 10^{-3}$ g ml$^{-1}$ was negative for all of the samples and increased with increasing $x_H$. By linear extrapolation from the higher concentration range to $c = 0$, the free diffusion coefficient, $D_{os}$, was obtained and hence (using the well-known

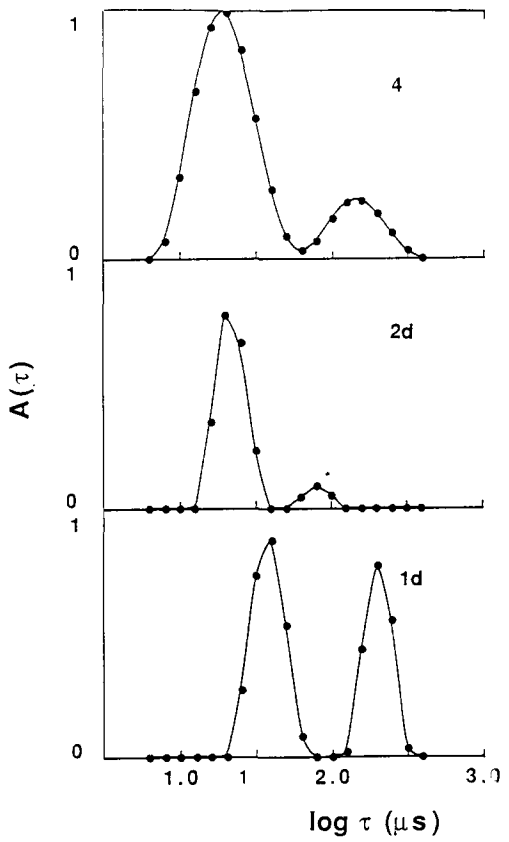


**Figure 1** Relaxation time distribution, $A(\tau)$, as obtained by Laplace inversion of autocorrelation functions by means of CONTIN for samples indicated in the right-hand portion of the figures

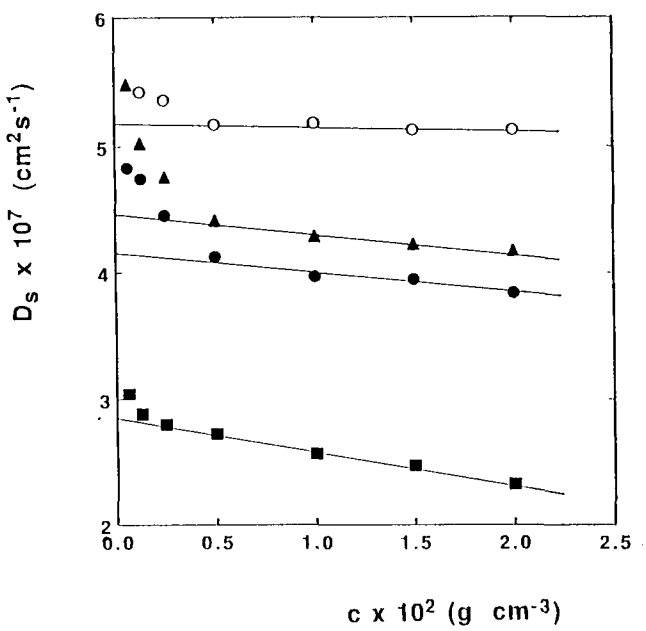


**Figure 2** Concentration dependence of the diffusion coefficient $D_s$ of copolymer solutions in TRIS buffer as obtained from dynamic light scattering data. Samples: ■, 1d; ●, 2d; ▲, 3; ○, 4

Stokes–Einstein formula) the hydrodynamic radius, $R_{hs}$ (*Table 2*).

The slow diffusion process was observed only for copolymers with $x_{NAp} \approx 7$ mol% (copolymers 1d, 2d, 3, 4). The concentration dependence of $D_l$ and $A_l/A_s$ (where $A_l$ and $A_s$ are the relative scattering amplitudes for slow and fast diffusion processes, respectively) are given for copolymer1d ($x_H = 0$ mol%) in *Figure 3*. Both the $A_l/A_s$ ratio and $D_l$ decreased as the concentration increased. In the case of copolymers 2d, 3 and 4 ($x_H \gtrsim 9$ mol%), both $D_l$ and $A_l/A_s$ were found to be independent of concentration within experimental error. The magnitude of $A_l/A_s$, with the exception of sample 1d, increased with increasing $x_H$ (*Table 2*). The values of $R_{hl}$, corresponding to slow diffusion processes, are also given in *Table 2* for the sake of comparison.

Integral light scattering data for copolymers with $x_{NAp} \approx 7$ mol% (copolymers 1d, 2d, 3, 4) are shown in *Figure 4*. The $Kc/\Delta R(0)$ ratio increased with increasing $x_H$, in analogy with the $D_s$ values. Total molar mass ($M_w^t$) values obtained by extrapolation from the higher concentration range gave the weight-average molar mass for all major types of aggregates in a particular system;

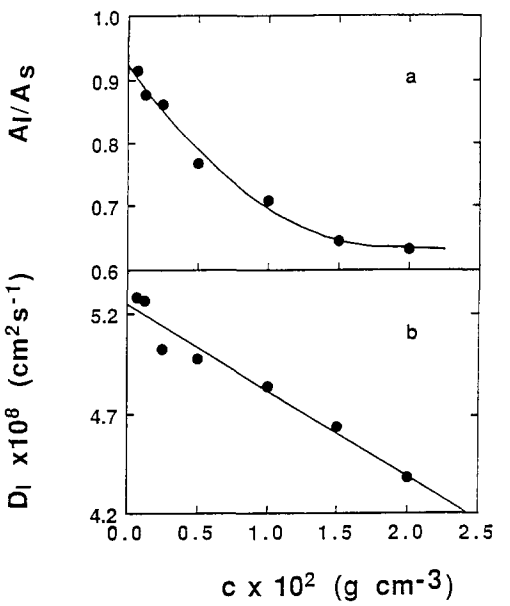


**Figure 3** Plots of (a) the scattering amplitude ratios $A_l/A_s$ and (b) the diffusion coefficient $D_l$ for the slow mode as a function of concentration $c$; sample 1d

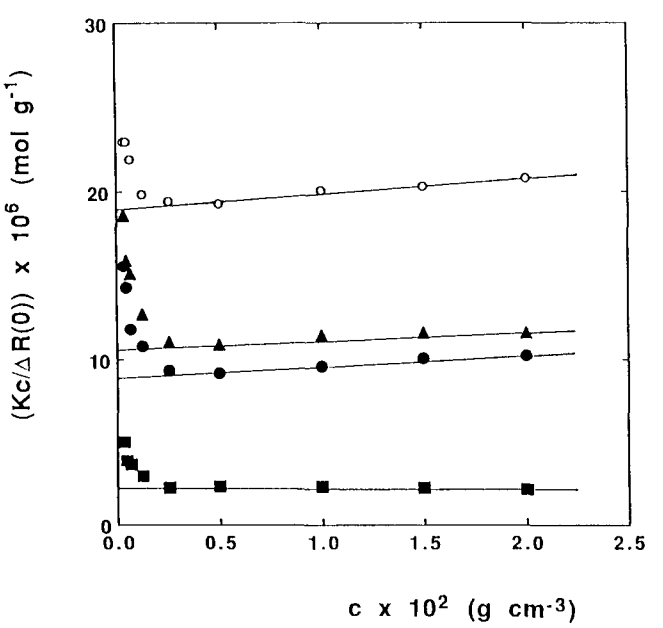


**Figure 4** Concentration dependence of $Kc/\Delta R(0)$ of copolymer solutions in TRIS buffer as determined from light scattering data. Samples: ■, 1d; ●, 2d; ▲, 3; ○, 4

$M_w^t$ decreased with increasing $x_H$ (*Table 2*). The second virial coefficient, $A_2$, which was calculated from the higher concentration range measurements ($c > 0.25$ g ml$^{-1}$), was zero for copolymer 1d ($x_H = 0$ mol%) and positive for samples 2d, 3, 4 with $x_H \gtrsim 9$ mol% (*Table 2*). The $A_2$ values increased with increasing $x_H$, reflecting the increased solubility of the corresponding copolymers (*Table 2*). The increase in $Kc/\Delta R(0)$ values at low concentrations with decreasing concentration (*Figure 4*) coincided with increases in $D_s$, as shown in *Figure 2*.

The effects of the hydrophobic side-chain content ($x_{NAp}$) on the solution properties of HPMA copolymers are summarized in *Table 2*. $A_2$ values increased with decreasing $x_{NAp}$ and increasing $x_H$, reflecting an increase in the water solubility of the copolymers. The association number $n$, calculated using the molecular weight data in *Tables 1* and *2* decreased with decreasing $x_{NAp}$. The higher value of $n$ in copolymers with $x_{NAp} \leqslant 2.7$ mol%, and containing HEPES side-chains (2–2d), than in those without HEPES (1–1b) confirmed the amphiphilic role of HEPES. The association number $n$ of samples 1d and 1b were higher than those of analogous samples in ref. 5. This discrepancy can be explained by the difference in copolymer preparation (discussed later).

The concentration dependence of $Kc/\Delta R(0)$ and $D_s$ for sample 2d ($x_H = 8.9$ mol% and $x_{NAp} = 6.5$ mol%) was typical of associated systems[13,14]. In such a system, micelles are formed by 'closed association', where unassociated copolymer molecules (unimers) are in dynamic equilibrium with spherical polymolecular micelles. The existence of the critical micelle concentration, $c_{mc}$, the concentration at which micelle formation begins, has been postulated for the closed association system. With an increasing concentration of solute, the equilibrium shifted towards the formation of polymolecular micelles. Polymeric association systems described in the literature are, typically, solutions of graft and block copolymers in selective solvents (i.e. liquids that are a good solvent for one block and a non-solvent for the other block)[13,14]. Besides these systems, micelle formation by amphiphilic side-chain polymers has been observed and investigated experimentally[15–24]. Recently, a microscopic model for the formation of micelles in these systems has been developed[25]. The system under study relates to these systems, but differs in an increase in emphasis of the role of the hydrophobic end-groups (*p*-nitroaniline). In agreement with our previous results[5], these copolymers formed micelles with *p*-nitroaniline oriented inside and hydrophilic polymer chains on the outside. The hydrophobicity of the end-groups of the side-chains seemed to be crucial in this case.

The changes in the solution behaviour of sample 2d ($x_H = 8.9$ mol% and $x_{NAp} = 6.5$ mol%) as its concentration decreased can be explained[13] by the decomposition of the micelles when approaching $c_{mc}$. As the concentration decreased, the dynamic equilibrium of the association process shifted in favour of the unimer form. The increase in unimer concentration upon dilution was manifested in an observed increase in both $D_s$ and $Kc/\Delta R(0)$. In the ideal case of a uniform copolymer, one would expect that at higher concentrations the equilibrium would shift towards the formation of micelles. Extrapolation from higher concentrations would then yield the micellar molar mass. However, distributions in the chemical composition of the copolymer could result in the presence of a fraction of molecules with a hydrophobic side-chain content so low that they would not take part in the association equilibrium. Such molecules would exist as unimers regardless of the experimental conditions. Thus, the $M_w^t$ value gives the weight-average molar mass for both micelles ($M_w^m$) and the unimer ($M_w^u$) and is generally smaller than the value for micelles alone. The ratio $n = M_w^t/M_w^u$ obtained from the data in *Tables 1* and *2* is also smaller than the true number of copolymer molecules in the micelles (association number)[5].

The same conclusions are essentially valid for copolymer 3 ($x_H = 18.2$ mol% and $x_{NAp} = 7.4$ mol%), since the contribution of the slow diffusion mode (larger aggregates) was still low ($A_1/A_s = 0.1$). In the case of copolymers 1d and 4, the contribution of the larger aggregates to the scattered light needed to be subtracted from the totally scattered light in order to obtain a reasonable approximation for the $M_w^m$ values for the smaller micelles. The association numbers of the micelles (lowest limit) of copolymers 1d and 4, which were calculated from $M_w^t$ values that were reduced using $A_1/A_s$ data, are shown in *Table 2*. It appears that the association number decreases with increasing $x_H$, in agreement with expectations.

The presence of larger aggregates cannot be explained by a simple association model. In an attempt to rationalize their existence, effects of temperature and solution pH on solution composition were evaluated. The temperature dependence of $D_s\eta/T$, where $\eta$ is the viscosity of solvent and $T$ the absolute temperature, is shown in *Figure 5*. $D_s$ values were multiplied by the factor $\eta/T$ to eliminate the direct effects of solvent viscosity and temperature changes. The cloud points are denoted in the figure by arrows, and the corresponding temperatures of macrophase separation, $T_c$, are given in *Table 2*. It can be seen that the $T_c$ of copolymer 1d (33.5°C) is close to room temperature; this could explain the presence of larger aggregates in the solvent measured at room temperature (22°C). The larger aggregates were probably created by a partial phase separation of the copolymer molecules with higher than average amount

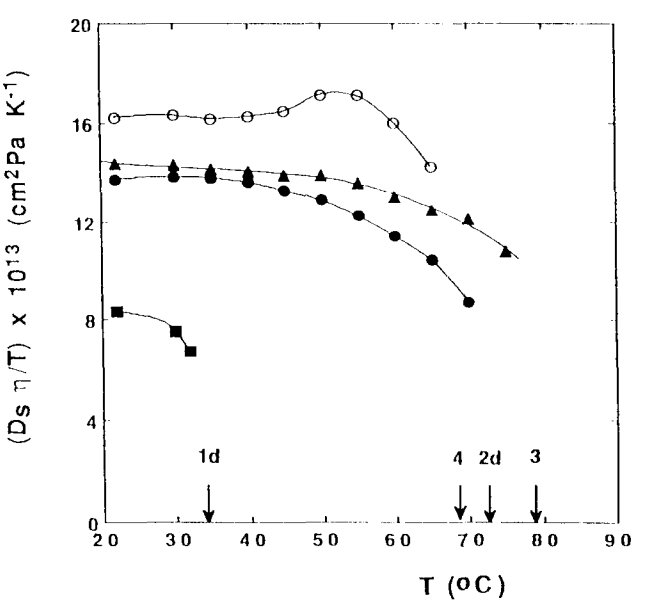


**Figure 5** Temperature dependence of the diffusion coefficient $D_s$ ($c = 1 \times 10^{-2}$ g ml$^{-1}$) of copolymers with high content of hydrophobic side-chains ($x_{NAp} \approx 7$ mol%) in TRIS buffer. Samples: ■, 1d; ●, 2d; ▲, 3; ○, 4. Cloud points are denoted by arrows

of hydrophobic side-chains, which arose as a consequence of the chemical inhomogeneity in the molecules.

The $T_c$s of copolymers 1–1d are about 10°C higher than those of the copolymers studied earlier[5] (e.g. copolymer 3a in ref. 5). This difference can be attributed to the different synthetic procedures used in these studies. Whereas copolymers 1–1d were synthesized by direct copolymerization, the copolymers in ref. 5 were prepared by a two-step process. First, a reactive HPMA copolymer precursor was prepared, followed by a polymer-analogous attachment of phenylalanine *p*-nitroanilide. However, during the latter procedure a small part of reactive *p*-nitrophenyl ester groups was hydrolysed. Consequently, the copolymers used in ref. 5 contain a small amount of side-chains terminated in ionizable carboxyl groups. Their presence appears to be the reason for the slight increase in $T_c$.

The addition of amphiphilic side-chains of AHEPES substantially increased the solubility of the copolymers. This was reflected in their higher $T_c$s. As expected, there was also a distinct decrease in the $D_s\eta/T$ values in the vicinity of $T_c$ due to an increase in the dimensions of the aggregates induced by a decrease in the thermodynamic quality of the solvent. While the $D_s\eta/T$ values for copolymers 2d and 3 are essentially independent of temperature at temperatures significantly above or below $T_c$, a small increase for $D_s\eta/T$ can be observed between 40 and 55°C for copolymer 4. This effect probably indicates a collapse in the coils of the flexible polymers in a thermodynamically poor solvent induced by approaching the Flory Θ-temperature[26].

As for the slow diffusion mode, $D_l\eta/T$ was essentially independent of temperature within experimental error, and $A_l/A_s$ decreased monotonically with increasing temperature to 0.05 for copolymer 3 (results not shown). The results obtained for copolymer 4 are shown in *Figure 6*, which shows that $D_l$ increased faster than $T/\eta$ at $T>40$°C. At the same time, $A_l/A_s$ decreased. It can be concluded that both the micelle concentration and size decreased with increasing temperature at temperatures higher than 40°C. In other words, the particles were destabilized at higher temperatures. Thus, smaller aggregates are favoured in a thermodynamically poor solvent for HPMA copolymers.

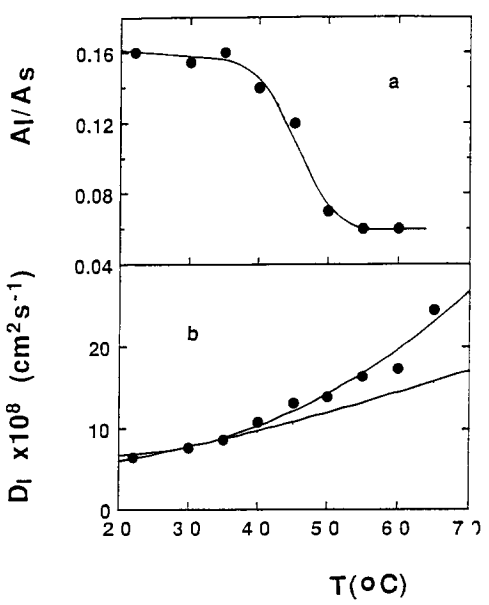


**Figure 6** Plots of (a) the scattering amplitude ratios $A_l/A_s$ and (b) the diffusion coefficient $D_l$ as a function of temperature for sample 4

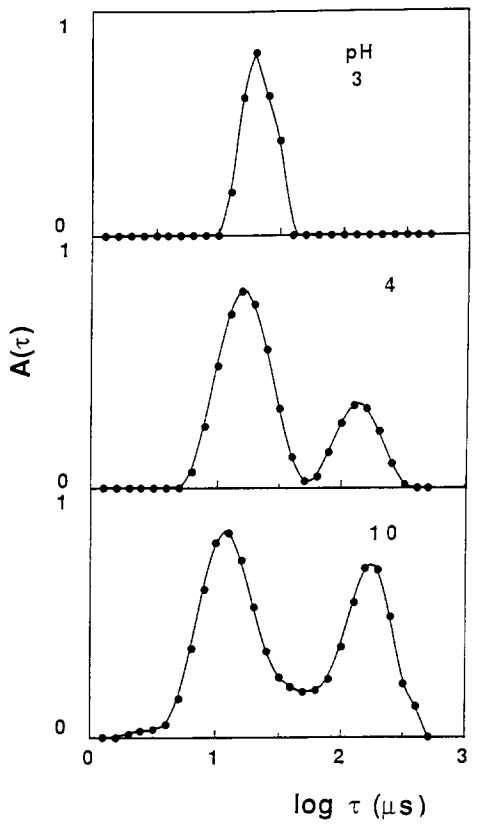


**Figure 7** Relaxation time distribution, $A(\tau)$, for copolymer 4 at different pH values

**Table 3** Dependence of solution properties of copolymer 4 on pH

| pH | $M_w^{app}\times10^{-4}$ [a] | $D_s\times10^7$ ($cm^2\,s^{-1}$) | $D_l\times10^8$ ($cm^2\,s^{-1}$) | $A_l/A_s$ |
|---|---|---|---|---|
| 3[b] | 8.7 | 5.04 | – | 0 |
| 4[b] | 8.4 | 4.71 | 5.69 | 0.11 |
| 6[c] | 5.5 | 5.25 | 6.41 | 0.12 |
| 8[c] | 4.1 | 6.27 | 7.46 | 0.36 |
| 8[d] | 5.0 | 5.20 | 6.80 | 0.22 |
| 10[e] | 2.9 | 8.36 | 6.73 | 0.68 |

[a] $M_w^{app}=\Delta R(0)/Kc$ for $c=0.01\ g\,ml^{-1}$
Buffers:
[b] Potassium hydrogen phthalate
[c] Potassium dihydrogen phosphate
[d] TRIS
[e] Sodium bicarbonate

The effect of solvent pH on the decay time distribution, $A(\tau)$, for copolymer 4 is shown in *Figure 7* (the scattering angle $\theta=90°$, $c=0.01\ g\,ml^{-1}$). The most striking effect is the strong pH dependence of the relative scattering intensity of the slow diffusion mode; $A_l/A_s$ decreased with decreasing pH (*Table 3*). The larger aggregates essentially disappeared at pH = 3. It can be seen in *Table 3* that the $M_w^{app}$ ($=\Delta R(0)/Kc$ for $c=0.01\ g\,ml^{-1}$), $D_s$ and $D_l$ values were influenced by pH. Both $D_s$ and $D_l$ values decreased with decreasing pH. In contrast, the $M_w^{app}$ values increased with decreasing pH. Hence, the density of the aggregates increased with decreasing pH.

The observed effect of pH on the solution properties of copolymer 4 ($x_H=35.9$ mol% and $x_{NAp}=6.8$ mol%) could be explained qualitatively by the well-known

electrolyte behaviour of AHEPES molecules[9]. Moreover, it was suspected that the amphiphilic properties of the AHEPES side-chains contributed to the formation of the micelles at low concentrations in aqueous solutions. This was corroborated by preliminary experiments conducted with the AHEPES homopolymer ($x_H = 100$ mol%). The association behaviour was investigated, and micelles with $R_h = 130$ nm were detected (results not shown). Therefore, the larger aggregates observed in the d.l.s. experiments were probably micelles resulting from the association of AHEPES monomer units. Indeed, the d.l.s. measurements at pH = 10 (*Figure 7*) provided a good example of such association. When the pH is decreased to the half-neutralization point (pH = 7.1), the HEPES molecule forms a zwitterionic structure[9]. The consequence of this in AHEPES-containing copolymers is a decrease in both solubility and amphiphilicity. This should result partially in a decrease in the concentration of larger micelles (it implies a decrease in $A_l/A_s$) and partially in the formation of new smaller micelles arising from hydrophobic interactions of the hydrophobic *p*-nitroaniline-containing side-chains. A limiting case of this phenomenon are the small compact micelles ($n \approx 6$) found at the solubility limit at pH = 3. These findings are in concurrence with the results of the temperature measurements of d.l.s. where only one type of small aggregates was observed at higher temperatures. At these temperatures the TRIS buffer is a thermodynamically poor solvent for the copolymer (*Figure 6*). Thus, an increase in temperature and/or decrease of the pH can produce analogous changes in solution behaviour.

## CONCLUSIONS

The objective of this study was to increase the water solubility of HPMA copolymers containing hydrophobic side-chains to enable the incorporation of larger amounts of hydrophobic drugs into the polymer structure. To this end, AHEPES comonomer was incorporated into the HPMA copolymers. This comonomer substantially increased the water solubility of the copolymers, but did not prevent the formation of micelles in aqueous solutions. The copolymers with a low content of hydrophobic *p*-nitroaniline-containing side-chains were soluble molecularly in aqueous solutions. HPMA copolymers with a high content of *p*-nitroaniline-containing side-chains associated in water and generally formed two types of micelles of different sizes. Micellization depended on hydrophobic and amphiphilic side-chain contents, polymer concentration, temperature and solvent pH. Thus, macromolecules with higher content of *p*-nitroaniline-containing side-chains and low content of HEPES side-chains tended to form small, compact micelles with hydrophobic *p*-nitroaniline molecules oriented into the core while macromolecules with a high content of HEPES side-chains tended to form large micelles. Incorporation of the AHEPES comonomer into the copolymer structure appeared to support the formation of large micelles due to its amphiphilic nature. The formation of large micelles was found to be strongly dependent on solvent pH due to the electrolyte behaviour of AHEPES monomer units. The solution behaviour of the copolymers reflected the competition between these two association processes. The coexistence of two types of micelles in solution probably results from the chemical inhomogeneity of the copolymer macromolecules.

## ACKNOWLEDGEMENTS

The work was supported in part by a gift from Insutech, Inc., Salt Lake City, Utah. The authors thank Dr E. Mack for valuable discussions. Č. K. thanks the Institute of Macromolecular Chemistry, Czech Academy of Sciences for leave of absence and the University of Utah for granting a Visiting Associate Professorship.

## REFERENCES

1 Ringsdorf, H. in 'Drug Carriers in Biology and Medicine' (Ed. G. Gregoriadis), Academic Press, London, 1979
2 de Duve, C., de Barsy, T., Poole, B., Trouet, A., Tulkens, P. and van Hoof, F. *Biochem. Pharmacol.* 1974, **23**, 2495
3 Kopeček, J. *J. Controlled Release* 1990, **39**, 1125
4 Bader, M., Ringsdorf, H. and Schmidt, B. *Angew. Makromol. Chem.* 1984, **123/124**, 457
5 Ulbrich, K., Koňák, Č., Tuzar, Z. and Kopeček, J. *Makromol. Chem.* 1987, **188**, 1261
6 Nukui, M., Hoes, K., van den Berg, H. and Feijen, J. *Makromol. Chem.* 1991, **192**, 2925
7 Ambler, E. L., Brookman, L., Brown, J., Goddard, P. and Petrak, K. *J. Bioact. Comp. Polym.* 1992, **7**, 223
8 Strohalm, J. and Kopeček, J. *Angew. Macromol. Chem.* 1978, **70**, 109
9 Mulvaney, J. E., Cutler, R. S. and Jensen, R. G. *J. Polym. Sci., Polym. Lett. Edn* 1981, **19**, 103
10 Kopeček, J. *Makromol. Chem.* 1977, **178**, 2169
11 Tuzar, Z. and Kratochvíl, P. *Collect. Czech. Chem. Commun.* 1976, **32**, 3358
12 Provencher, S. W. *Makromol. Chem.* 1979, **180**, 201
13 Tuzar, Z. and Kratochvíl, P. *Adv. Colloid Interface Sci.* 1976, **6**, 201
14 Tuzar, Z. and Kratochvíl, P. in 'Surface and Colloid Science Series' Vol. 15 (Ed. E. Matijevic), Plenum Press, New York, 1993, p. 1
15 Finkelmann, H., Luhmann, B. and Rehage, G. *Colloid Polym. Sci.* 1982, **260**, 56
16 Luhmann, B., Finkelmann, H. and Rehage, G. *Angew. Makromol. Chem.* 1984, **123**, 217
17 Sonnessa, A. J., Cullen, W. and Ander, P. *Macromolecules* 1980, **13**, 195
18 Knapick, E. G., Hirsch, J. A. and Ander, P. *Macromolecules* 1985, **18**, 1015
19 Shih, L. B., Sheu, E. Y. and Chen, S. H. *Macromolecules* 1988, **21**, 1387
20 Schulz, D. N., Kaladas, J. J., Maurer, J., Bock, J., Pace, S. J. and Schulz, W. W. *Polymer* 1987, **28**, 2110
21 Valint, P. L., Jr. and Bock, J. *Macromolecules* 1988, **21**, 175
22 Pietschmann, N., Brezesinski, G., Tschierske, C., Zaschke, H. and Kuschel, F. *Liquid Crystals* 1989, **5**, 1697
23 Lee, J. H., Kopečková, P., Kopeček, J. and Andrade, J. D. *Biomaterials* 1990, **11**, 455
24 Lee, J. H., Kopeček, J. and Andrade, J. D. *J. Biomed. Mater. Res.* 1989, **23**, 351
25 Hamad, E. and Qutubuddin, S. *Macromolecules* 1990, **23**, 4185
26 Flory, P. J. 'Principles of Polymer Chemistry', Cornell University Press, Ithaca, 1975